Pesticide Biochemistry and Physiology 106 (2013) 85–92

Contents lists available at SciVerse ScienceDirect

Pesticide Biochemistry and Physiology

journal homepage: www.elsevier.com/locate/pest

Inhibitor profile of *bis*(*n*)-tacrines and *N*-methylcarbamates on acetylcholinesterase from *Rhipicephalus* (*Boophilus*) *microplus* and *Phlebotomus papatasi*

Daniel R. Swale [a], Fan Tong [a], Kevin B. Temeyer [b], Andrew Li [b], Polo C-H. Lam [c], Maxim M. Totrov [c], Paul R. Carlier [d], Adalberto A. Pérez de León [b], Jeffrey R. Bloomquist [a,*]

[a] Department of Entomology and Nematology, Emerging Pathogens Institute, University of Florida, Gainesville, FL 32611, USA
[b] Knipling-Bushland U.S. Livestock Insects Research Laboratory, United States Department of Agricultural-Agricultural Research Service, 2700 Fredericksburg Road, Kerrville, TX 78028, USA
[c] Molsoft LLC, 3366 North Torrey Pines Court, Suite 300, La Jolla, CA 92037, USA
[d] Department of Chemistry, Virginia Tech, Blacksburg, VA 24061, USA

ARTICLE INFO

Article history:
Available online 28 March 2013

Keywords:
Leishmaniasis
Sandfly
Cattle fever
Southern cattle tick
Insecticides
Selectivity

ABSTRACT

The cattle tick, *Rhipicephalus* (*Boophilus*) *microplus* (*Bm*), and the sand fly, *Phlebotomus papatasi* (*Pp*), are disease vectors to cattle and humans, respectively. The purpose of this study was to characterize the inhibitor profile of acetylcholinesterases from *Bm* (*Bm*AChE1) and *Pp* (*Pp*AChE) compared to human and bovine AChE, in order to identify divergent pharmacology that might lead to selective inhibitors. Results indicate that *Bm*AChE has low sensitivity (IC_{50} = 200 μM) toward tacrine, a monovalent catalytic site inhibitor with sub micromolar blocking potency in all previous species tested. Similarly, a series of *bis*(*n*)-tacrine dimer series, bivalent inhibitors and peripheral site AChE inhibitors possess poor potency toward *Bm*AChE. Molecular homology models suggest the r*Bm*AChE enzyme possesses a W384F orthologous substitution near the catalytic site, where the larger tryptophan side chain obstructs the access of larger ligands to the active site, but functional analysis of this mutation suggests it only partially explains the low sensitivity to tacrine. In addition, *Bm*AChE1 and *Pp*AChE have low nanomolar sensitivity to some experimental carbamate anticholinesterases originally designed for control of the malaria mosquito, *Anopheles gambiae*. One experimental compound, 2-((2-ethylbutyl)thio)phenyl methylcarbamate, possesses >300-fold selectivity for *Bm*AChE1 and *Pp*AChE over human AChE, and a mouse oral LD_{50} of >1500 mg/kg, thus providing an excellent new lead for vector control.

1. Introduction

Utilization of insecticides for disease vector control remains the most effective component of the integrated vector management approach for control of vector borne diseases [1]. The cattle tick, *Rhipicephalus* (*Boophilus*) *microplus* (Canestrini; *Bm*), is a potentially deadly pest of cattle, since it is a primary vector for babesiosis and anaplasmosis [2]. Economic losses are furthered substantially as normal feeding behavior of tick infestations lead to reduction in milk production and weight gain, as well as overall declines in cattle health [3]. Similarly, the sandfly, *Pp* is a primary vector of numerous zoonotic diseases significant to human health, including leishmaniasis and bartonellosis [4].

Control programs for these two disease vectors rely largely upon the use of insecticides. For control of the cattle tick, the USDA implemented CFTEP, which mandates a quarantine zone, dipping of all imported cattle into organophosphate (e.g. coumaphos) solutions, and a 7–14 day quarantine period [4–6]. Similarly, sandfly control is largely based on insecticides through the use of indoor residual spraying with pyrethroids and organophosphates, and the use of insecticide treated bednets is a successful and sustainable method for malaria control that has also been evaluated for control of Phlebotomine sandflies [7–11].

Abbreviations: AChE, Acetylcholinesterase; *Ag*, *Anopheles gambiae*; ATCh, acetylthiocholine iodide; *Bm*, *Rhipicephalus (Boophilus) microplus*; CFTEP, Cattle Fever Tick Eradication Program; CS, catalytic site; *Dm*, *Drosophila melanogaster*; DMSO, dimethyl sulfoxide; DTNB, 5,5'-dithiobis-(2-nitro)benzoic acid; *h*AChE, recombinant human AChE; IC_{50}, inhibitory concentration needed to inhibit 50% of the enzyme activity; OECD, Organization for Economic Co-operation and Development; OP, Organophosphate; *Pp*, *Phlebotomus papatasi*; PS, peripheral site; r*Bm*AChE1, recombinant *Boophilus microplus* acetylcholinesterase, isoform 1; r*Pp*AChE, recombinant *Phlebotomus papatasi* acetylcholinesterase; SR, selectivity ratio; *Tc*, *Torpedo californica*; USDA, United States Department of Agriculture.

* Corresponding author. Fax: +1 352 273 9420.
E-mail address: jbquist@epi.ufl.edu (J.R. Bloomquist).

0048-3575/$ - see front matter © 2013 Elsevier Inc. All rights reserved.
http://dx.doi.org/10.1016/j.pestbp.2013.03.005

Report Documentation Page

Form Approved
OMB No. 0704-0188

1. REPORT DATE	2. REPORT TYPE	3. DATES COVERED
2013		**00-00-2013 to 00-00-2013**

4. TITLE AND SUBTITLE	5a. CONTRACT NUMBER
Inhibitor profile of bis(n)-tacrines and N-methylcarbamates on acetylcholinesterase from Rhipicephalus (Boophilus) microplus and Phlebotomus papatasi	5b. GRANT NUMBER
	5c. PROGRAM ELEMENT NUMBER
6. AUTHOR(S)	5d. PROJECT NUMBER
	5e. TASK NUMBER
	5f. WORK UNIT NUMBER
7. PERFORMING ORGANIZATION NAME(S) AND ADDRESS(ES) **University of Florida,Department of Entomology and Nematology,Emerging Pathogens Institute,Gainesville,FL,32611**	8. PERFORMING ORGANIZATION REPORT NUMBER
9. SPONSORING/MONITORING AGENCY NAME(S) AND ADDRESS(ES)	10. SPONSOR/MONITOR'S ACRONYM(S)
	11. SPONSOR/MONITOR'S REPORT NUMBER(S)

12. DISTRIBUTION/AVAILABILITY STATEMENT
Approved for public release; distribution unlimited

13. SUPPLEMENTARY NOTES

14. ABSTRACT

The cattle tick, Rhipicephalus (Boophilus) microplus (Bm), and the sand fly, Phlebotomus papatasi (Pp), are disease vectors to cattle and humans, respectively. The purpose of this study was to characterize the inhibitor profile of acetylcholinesterases from Bm (BmAChE1) and Pp (PpAChE) compared to human and bovine AChE, in order to identify divergent pharmacology that might lead to selective inhibitors. Results indicate that BmAChE has low sensitivity (IC50 = 200 lM) toward tacrine, a monovalent catalytic site inhibitor with sub micromolar blocking potency in all previous species tested. Similarly, a series of bis(n)-tacrine dimer series, bivalent inhibitors and peripheral site AChE inhibitors possess poor potency toward BmAChE. Molecular homology models suggest the rBmAChE enzyme possesses a W384F orthologous substitution near the catalytic site, where the larger tryptophan side chain obstructs the access of larger ligands to the active site, but functional analysis of this mutation suggests it only partially explains the low sensitivity to tacrine. In addition, BmAChE1 and PpAChE have low nanomolar sensitivity to some experimental carbamate anticholinesterases originally designed for control of the malaria mosquito Anopheles gambiae. One experimental compound, 2-((2-ethylbutyl)thio)phenyl methylcarbamate, possesses >300-fold selectivity for BmAChE1 and PpAChE over human AChE, and a mouse oral LD50 of >1500 mg/kg, thus providing an excellent new lead for vector control.

15. SUBJECT TERMS

16. SECURITY CLASSIFICATION OF:			17. LIMITATION OF ABSTRACT	18. NUMBER OF PAGES	19a. NAME OF RESPONSIBLE PERSON
a. REPORT	b. ABSTRACT	c. THIS PAGE			
unclassified	**unclassified**	**unclassified**	**Same as Report (SAR)**	**8**	

Although these control methods have been effective in reducing *Boophilus* and *Phlebotomus* populations, control has become increasingly difficult due to escalating insecticide resistance among wild populations [5,12–14]. OP insecticides, such as coumaphos, are inhibitors of AChE (EC 3.1.1.7), a serine hydrolase responsible for terminating nerve signals at the synapses of cholinergic systems within the central nervous system of invertebrates, leading to death [15]. OP and pyrethroid resistance has been attributed to both metabolic and target site mechanisms, with the latter being the primary reason for OP resistance [12,16–19]. OP-insensitive AChE might provide cross resistance to insecticides with similar mode of action, such as carbamates. Modification of current compounds can provide increased invertebrate/vertebrate selectivity ratios alongside the potential for development of resistance-mitigating compounds.

The three-dimensional crystal structures of AChE from *Tc* [20], *Dm* [21], and mouse [22] (among others) are available, and provide insights on structure–function relationships for numerous inhibitors. Pharmacological and structural analyses of AChE have revealed that AChE contains two binding sites for inhibitors: one at the CS and one near the entrance to the catalytic gorge, the PS [20–22]. The CS is located about 4 Å from the base of the gorge and is defined (in part) by the catalytic triad S200, H440, E327, as well as W84 (*Tc* numbering), the latter serving to bind the trimethylammonium group of acetylcholine [23]. In turn, the PS is located toward the mouth of the gorge and consists of W279, Y70, D72, and Y121 (*Tc* numbering) [24–27]. The PS has been shown to briefly bind substrates en route to the CS, thereby increasing catalytic efficiency [24,25]. Using differences in CS geometry between *Ag*AChE and *h*AChE, we have developed anticholinesterase mosquitocides (carbamates) having mosquito selectivity of up to 500-fold [28]. Simultaneous occupancy of the CS and PS sites through the design of bivalent inhibitors should facilitate the mitigation of AChE target site resistance, since resistance to this type of compound would require the development of multiple mutations in the protein while retaining sufficient functionality.

In this study, we characterized the inhibitor profile of acetylcholinesterases from r*Bm*AChE1 and *Pp*AChE compared to human and bovine AChE, in order to identify divergent pharmacology that might lead to selective inhibitors. Secondly, we show evidence of highly potent and selective experimental carbamate inhibitors that can assist in the control of *Bm* and *Pp* populations.

2. Methods

2.1. Inhibitors, solvents, and assay reagents

Propoxur (purity ⩾ 99%), bendiocarb (purity ⩾ 99%), edrophonium (purity ⩾ 98%), eserine (purity ⩾ 99%), and tacrine (purity ⩾ 99%) were purchased from Sigma–Aldrich (St. Louis, MO, USA). Experimental carbamates (Fig. 1) were prepared as described in Carlier et al. [28]. All experimental compounds were purified by column chromatography and/or re-crystallization, and were >95% pure by ^{1}H NMR analysis. Carbamate and tacrine-based inhibitors used in this study are shown in Fig. 1. *Bis*(*n*)-tacrine dimers (*n* = 2, 3, 4, 5, 6, 7, 8, 9, 10, and 12 methylenes) were synthesized and purified to >95% using established procedures [29]. The inhibitors donepezil (⩾98% purity), BW284c51 (⩾98% purity), tubocurarine (>97% purity), and ethidium (95% purity) were all purchased from Sigma–Aldrich (St. Louis, MO, USA). Ellman assay [30] reagents are composed of ATCh (⩾99% purity), DTNB (99% purity), and sodium phosphate buffer, all of which were purchased from Sigma–Aldrich (St. Louis, MO, USA). Molecular sieve OP type 3 Å beads were purchased from Sigma (St. Louis, MO, USA) and were used to prevent water absorption within the DMSO stock.

2.2. Molecular homology modeling

Homology model of the *Bm*AChE1 was constructed in ICM [31]. X-ray structure from the Protein Data Bank (PDB ID 1ACJ – the complex of *Torpedo Californica* AChE with tacrine) was used as a template. Side-chain refinement was performed in ICM using a Biased Probability Monte–Carlo (BPMC) global optimization procedure [32].

2.3. Enzyme preparations

Recombinant constructs of *R.* (*B.*) *microplus Bm*AChE1 (Table 1) were produced as previously described [33], except that baculovirus supernatants containing rBmAChE1 were produced in sf21 insect cell culture grown in Gibco® Sf-900™ III SFM (serum-free medium, Life Technologies, Carlsbad, CA). Site-directed mutagenesis was utilized to convert the codon for W384 to F384 (W384F) in cDNA of *BmAChE1* (Deutch #5, wt) pre-cloned into the baculoviral transfer plasmid pBlueBac4.5/B5-His-TOPO® (Life Technologies) as previously described [35]. Briefly, 5′-phosphorylated PCR primers *Bm*AChE1-1203U29X (CTTCTTCTTGCAATACTTCTTCGGATTTC) and *Bm*AChE1-1181L22 (GAACCTTCGTTTGCGTTAGAAC) were utilized (25 cycles, 66 °C annealing temp, 4 min extension at 72 °C) with the Phusion® Site-Directed Mutagenesis Kit (Thermo Fisher Scientific, Pittsburg, PA) to perform targeted mutagenesis following the instructions of the manufacturer. The mutagenized plasmid was transformed into *Escherichia coli* TOP10 chemically competent cells, sequence verified, and co-transfected with Bac-N-Blue™ DNA into Sf21 insect cells as previously described [35]. Baculovirus cultures were produced in sf21 cells grown in Gibco Sf-900™ III SFM. Baculoviral DNA was isolated and sequenced from all expression cultures to verify construction and expression of the intended coding sequences.

Six enzymes were utilized in this study: r*Bm*AChE1 and mutated r*Bm*AChE1 (W384F), prepared as described above, r*Pp*AChE, *h*AChE, bovine brain homogenate, and *Ag*AChE homogenate. *Ag*AChE and bovine brain homogenate enzyme was prepared from groups of ten whole non-blood fed adult female mosquitoes or

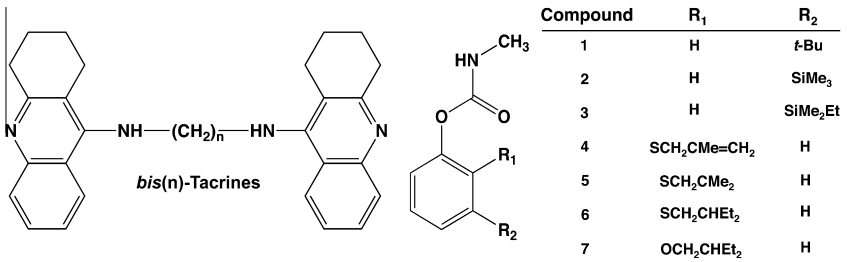

Compound	R_1	R_2
1	H	*t*-Bu
2	H	$SiMe_3$
3	H	$SiMe_2Et$
4	$SCH_2CMe{=}CH_2$	H
5	SCH_2CMe_2	H
6	SCH_2CHEt_2	H
7	OCH_2CHEt_2	H

Fig. 1. Structure of *bis*(*n*)-tacrines, where *n* = 2, 3, 4, 5, 6, 7, 8, 9, 10, and 12 methylenes, as well as the experimental methylcarbamate inhibitors used in this study.

Table 1
Amino acid substitutions[a] in recombinant BmAChE1 constructs of *R.* (*B.*) *microplus*.

BmAChE1 Amino acid Substitution	(wt) Deutch #5 (OP-S)	Muñoz #4 (OP-S)	San Roman #4 (OP-R)	San Roman #11 (OP-R)	Tuxpan #11 (OP-R)	Tuxpan #17 (OP-R
E55G			X			
E60 K	X	X	X	X	X	X
P78T	X	X	X	X	X	X
P157S			X	X		
D188G					**X**	
E196G					**X**	
T219A	X	X	X	X	X	X
E238G	X	X			X	X
A260T	X	X	X	X	X	X
V331A		**X**			**X**	**X**
N333S			X			
A349 V	X	X	X	X	X	X
T362A				X		
K364R	X	X			X	X
F390S		**X**			**X**	**X**
M426 V	X	X			X	X
T437A	X	X			X	X
Q488R				X		
I493T				X		
Q497R			X			
R549H	X	X	X	X	X	X
E552Q	X	X			X	X
N566D						**X**
W571F			X	X		
T576A	X	X			X	X
N583D	X	X			X	X
P590A						**X**

[a] Amino acid substitutions compared to GenBank accession CAA11702 are indicated below each recombinant construct expressed in the baculovirus system. Bold underline type indicates substitutions present only in constructs described in more detail elsewhere [34], along with sensitivity to coumaphos-oxon (Table 5).

5 mg (wet weight) of excised bovine brain tissue. Bovine tissue collection was via a local slaughterhouse, and approved by the University of Florida IACUC. Each tissue was homogenized in 1 mL of ice-cold sodium phosphate buffer (0.1 M, pH 7.8) containing 0.3% Triton x-100, with an electric motor driven glass tissue homogenizer. The homogenate was centrifuged at 5000*g* using a Sorvall Fresco refrigerated centrifuge, at 4 °C for 5 min. The supernatant was used as the enzyme source for the assay. Prior to use, r*Bm*AChE1 and *Pp*AChE were diluted 10× and *h*AChE was diluted 100× with the aforementioned buffer + Triton mixture.

2.4. Enzyme inhibition assays

IC_{50} values were determined using slight modifications from Ellman et al. [30], as outlined in Hartsel et al. [28]. Briefly, 10 μL of enzyme solution was added to each well of a 96-well microtiter plate, along with 20 μL of dissolved compound and 150 μL of ice-cold phosphate buffer. The assay plate was incubated at 25 °C for 10 min. Ellman assay reagents, ATCh (0.4 mM, final concentration) and DTNB (0.3 mM, final concentration) were prepared fresh, and 20 μL was added to the enzyme to initiate the reaction. Changes in absorbance were recorded by a DYNEX *Triad* spectrophotometer (DYNEX Technologies, Chantilly, VA, USA) at 405 nm. Six inhibitor concentrations were used in triplicate to construct concentration–response curves. Inhibitors were dissolved in DMSO and stocks were diluted to give a final concentration of 0.1% DMSO (*v*/*v*) in the microtiter plate for each inhibitor concentration. Enzyme concentrations used were within the linear range of activity, therefore eliminating the need for protein quantification.

2.5. Mammalian toxicity studies

We performed a toxicity screen of three experimental carbamate insecticides **1**, **6**, and **7** using the OECD approved method, known as the "up-and-down method" [36], for oral dosing of male *Mus musculus* (ICR strain). The University of Florida IACUC approved all procedures for these experiments. Standard oral treatments used olive oil mixtures (≤400 μL) administered through a gavage needle. A maximum of eight mice total were used for each inhibitor and were monitored every 4 h for 24 h after the administration of the insecticide. Toxicity was recorded at 24 h post exposure. The mice were sacrificed at any sign of suffering and counted as dead.

2.6. Statistical analyses

Individual IC_{50} values were calculated using nonlinear regression with GraphPad Prism™ (GraphPad Software, San Diego, CA, USA). All experiments yielded acceptable Hill slope (>0.8) and r^2 (⩾0.99) values. IC_{50} values are expressed as mean of $n = 3$ values. Mean IC_{50} values and 95% confidence limits were determined with GraphPad InStat™ (GraphPad Software, San Diego, CA, USA). The mean IC_{50} values were statistically analyzed using an unpaired *t*-test (two tail) and Tukey's post-test with significance being represented by $P < 0.05$. Statistical analyses were performed using InStat™ (GraphPad Software, San Diego, CA, USA). Selectivity ratios of enzymes were determined by the equation: vertebrate IC_{50}/invertebrate IC_{50}. Estimates of murine LD_{50} values were calculated in the SAS statistical program (Cary, NC).

3. Results

3.1. Potency of AChE inhibitors in arthropods

The majority of compounds used for enzyme characterization act at the CS of AChE. Coumaphos oxon is a potent anticholinesterase against r*Bm*AChE (Table 2), but is 43-fold less effective against r*Pp*AChE (Table 2). Commercial carbamate insecticides (propoxur, carbaryl, and bendiocarb) are highly potent inhibitors of both r*Bm*AChE1 and r*Pp*AChE (Table 2). For both r*Bm*AChE and r*Pp*AChE,

Table 2
IC_{50} values of AChE inhibitors with enzymes utilized in this study. IC_{50} values are expressed in nM and are shown as means (n = 3). Selectivity ratios (SR) are expressed as follows: SR^1 = Bovine AChE IC_{50}/r*Bm*AChE1 IC_{50}; SR^2 = *h*AChE IC_{50}/r*Bm*AChE1 IC_{50}; SR^3 = *h*AChE IC_{50}/r*Pp*AChE1 IC_{50}.

Compound	r*Bm*AChE1 IC_{50}, nM (95% CI)	r*Pp*AChE IC_{50}, nM (95% CI)	*h*AChE IC_{50}, nM (95% CI)	Bovine AChE IC_{50}, nM (95% CI)	SR^1	SR^2	SR^3
Coumaphos oxon	10 (2–17)	430 (349–511)	111 (103–121)	1038 (875–1201)	104	11	0.26
Propoxur	33 (20–46)	89 (50–126	1442 (2430–3131)	1835 (1289–2381)	55	43	21
Carbofuran	5 (3–8)	8 (2–14)	38 (30–45)	73 (48–98)	15	8	5
Carbaryl	16 (5–27)	167 (126–208)	2780 (2430–3131)	2,605 (2343–2868)	163	174	17
Bendiocarb	16 (7–24)	15 (14–16)	182 (113–250)	195 (173–216)	12	11	12
Eserine	1.5 (0.5–2.5)	9 (4–14)	69 (54–84)	185 (145–224)	123	46	7.6
Edrophonium	2425 (1941–2910)	1178 (584–1771)	1081 (7774–1387)	1799 (1506–2091)	0.74	0.45	0.92
BW284C51	12,700 (12,400–13,000)	30 (20–39)	33 (18–46)	16 (11–21)	0.001	0.003	1.1
Tacrine	221,000 (171,000–270,000)	205 (168–240)	213 (122–304)	187 (143–229)	0.001	0.001	1.04
Donepezil	3% inhibition at 10^{-4}M	92 (69–114)	7 (3–10)	9 (4–13)	<0.001	<0.001	0.08
Tubocurarine	15% inhibition at 10^{-3}M	38,900 (31000–46700)	57,600 (48600–66600)	54,400 (49200–59600)	<0.05	<0.06	1.5
Ethidium	77,700 (68,300–87,000)	14,1006 (9391–18900)	22,900 (14600–31200)	32,300 (26300–38400)	0.42	0.3	1.6
1	37 (18–62)	10 (4–16)	233 (154–311)	259 (242–277)	7	6	23
2	190 (150–230)	22 (13–30)	539 (484–593)	1053 (896–12210)	5	3	25
3	364 (256–337)	16 (8–24)	451 (431–470)	1357 (1284–1430)	4	1	28
4	25 (10–39)	150 (90–209)	8035 (7743–8327)	6366 (6027–6704)	255	321	54
5	77 (56–96)	100 (73–126)	10,900 (10500–11400)	8955 (6055–12810)	116	142	109
6	15 (3–26)	14 (11–15)	5,127 (4871–5383)	5073 (4772–5373)	338	342	366
7	312 (256–366)	184 (137–229)	113,000 (72,500–153,000,0)	92,000 (85,000–99,000)	295	360	611

the most active carbamate was carbofuran, whereas in the tick propoxur was the least active, and for the sandfly it was carbaryl. Although commercial carbamates yielded fairly similar inhibition potencies for both r*Pp*AChE and r*Bm*AChE, experimental carbamates possessed varying potencies against the two enzymes (Table 2). For r*Bm*AChE1, experimental carbamates possess an activity range of approximately 25-fold, with **6** and **3** being the most and least potent inhibitor, respectfully. Compound **1** is the most potent experimental carbamate with a *meta* positioned side chain by approximately 5- to 10-fold, compared to **2** and **3**, respectively. Compound **6** displayed the greatest potency for experimental inhibitors studied with an *ortho* positioned side chain. For r*Pp*AChE, experimental inhibitors displayed a range of 18-fold with **1** and **7** being the most and least potent inhibitors, respectfully (Table 2). The *meta*-substituted compounds were of similar high potency, with compound **6** the only *ortho* carbamate of similar activity. This compound was also equipotent against both r*Bm*AChE1 and r*Pp*AChE. r*Bm*AChE1 was found to have low sensitivity (IC_{50} = 221 μM) toward tacrine, a monovalent CS inhibitor with sub micromolar blocking potency in all previous species tested, including r*Pp*AChE. Eserine, a natural product CS-directed inhibitor was the most potent compound tested in this study, and its activity favors r*Bm*AChE1 over r*Pp*AChE by a factor of six (Table 2). Edrophonium, a reversible CS inhibitor, was considerably less potent than the carbamates, and displayed similar mean IC_{50} values in the low micromolar range against r*Bm*AChE1 and r*Pp*AChE (Table 2).

The two peripheral site inhibitors studied (tubocurarine and ethidium) displayed poor inhibition of r*Bm*AChE1, but typical levels of inhibitory activity to r*Pp*AChE. Tubocurarine inhibited no more than 15% of enzyme activity at 1 mM with r*Bm*AChE1, and was roughly 25-fold more active against r*Pp*AChE (Table 2). Ethidium was more active than tubocurarine in both species, and showed 5-fold greater potency for r*Pp*AChE than r*Bm*AChE.

Bivalent AChE inhibitors spanning both the CS and PS binding domains possessed reduced inhibition potency toward r*Bm*AChE1 and high potency toward r*Pp*AChE. BW284c51 was active at the low micromolar level on r*Bm*AChE1, and was found to have 424-fold greater activity against r*Pp*AChE (Table 2). Donepezil showed approximately three percent inhibition at 100 μM, and was therefore considered to be inactive on r*Bm*AChE1. However, Donepezil was a potent inhibitor of r*Pp*AChE, as it was found to have an IC_{50} value of ca. 100 nM (Table 2). To further understand the inhibitor profile of r*Bm*AChE1 and r*Pp*AChE, the enzymes were also studied using a *bis*(n)-tacrine dimer series as structural probes to measure the distance between the CS and PS (Table 3). r*Pp*AChE was found to be more sensitive to the entire tacrine dimer series when compared to r*Bm*AChE1. Comparing IC_{50} values across r*Bm*AChE1 and r*Pp*AChE, the differences in potency ranged from 297-fold for *bis*(8)-tacrine to 1493-fold for *bis*(10)-tacrine (Table 3). For r*Bm*AChE1, the most potent tacrine dimer was found to be *bis*(8)-tacrine and the least potent was found to be *bis*(2)-tacrine. However, a different pattern of inhibition for r*Pp*AChE produced less than a 2.5-fold difference between *bis*(7)-tacrine through *bis*(12)-tacrine, with the IC_{50} values ranging from 2–5 nM (Table 3).

Table 3
Tacrine and tacrine dimer inhibition of tick and sandfly AChE.

Compound	r*Bm*AChE1 IC_{50} (nM; 95% CI)	*Pp*AChE IC_{50} (nM; 95% CI)
Tacrine	221,000 (171,000–270,000)	205 (168–240)
Bis(2)-tacrine	190,000 (162,000–218,000)	151 (132–166)
Bis(3)-tacrine	132,000 (120,000–156,000)	139 (100–161)
Bis(4)-tacrine	45,700 (33,600–56,400)	103 (87–128)
Bis(5)-tacrine	11,700 (9,061–15,900)	25 (15–36)
Bis(6)-tacrine	9421 (6209–13,017)	9 (5–15)
Bis(7)-tacrine	2919 (2198–3675)	5 (2–8)
Bis(8)-tacrine	892 (510–1109)	3 (0.5–6)
Bis(9)-tacrine	2046 (1,495–2583)	3 (0.5–5)
Bis(10)-tacrine	2986 (2687–3384)	2 (0.3–5)
Bis(12)-tacrine	4126 (3368–4892)	3 (0.6–6)

3.2. Potency of AChE inhibitors in mammals

The two mammalian AChE enzymes studied, human and bovine, displayed similar inhibition potencies to CS-directed compounds, with the largest potency difference being ca. 10-fold to coumaphos oxon (Table 2). Commercial carbamate inhibitors also displayed little difference in potency values to the mammalian AChE enzymes, with the largest difference being 1.9-fold (carbofuran). The most and least potent commercial CS inhibitors were found to be carbofuran and carbaryl, respectively, for both mammalian enzymes. Similarly, the experimental carbamates displayed little difference in IC_{50} values. The largest difference between the two mammalian species was 3-fold (**3**), and the potency ratios of most inhibitors neared unity. The most potent experimental carbamate for both enzymes was **1** (*meta*-substituted). A 2.7-fold

difference was observed in potency with eserine, the second most potent CS inhibitor, with *h*AChE more sensitive than bovine AChE. Edrophonium was found to be a low micromolar inhibitor to both mammalian enzymes, and *h*AChE was 1.6-fold more sensitive when compared to bovine (Table 2).

Mammalian enzymes were also found to possess similar sensitivities to both peripheral site inhibitors studied (Table 2). The potency differences between the two species was 1.05-fold and 1.4-fold for tubocurarine and ethidium, respectfully. Ethidium was found to be more potent than tubocurarine to both enzymes by approximately 2-fold.

Bivalent inhibitors, donepezil and BW284c51, were shown to be the most potent blockers of both mammalian enzymes, with IC_{50} values in the 7–33 nM range (Table 2). Donepezil was the most active inhibitor of both mammalian enzymes, with nearly equipotent IC_{50} values against *h*AChE bovine AChE. Although 2- to 4-fold less potent than donepezil, BW284c51 was still the second most potent inhibitor against *h*AChE and bovine AChE, with inhibition values differing by 2.1-fold across these species.

3.3. Inhibitor selectivity across mammals and arthropods

SR values are used to express *in vitro* selectivity differences between mammalian and arthropod enzymes, as shown in Table 2. For r*Bm*AChE1, the most selective standard carbamate was carbaryl when compared to both human and bovine enzymes. Otherwise, commercial carbamates were shown to have a range of enzyme selectivity that varied from 8- to 174-fold for *h*AChE and 12- to 163-fold for bovine AChE. Edrophonium was found to be negatively selective for both the human and bovine AChE enzymes, as they were more active on the mammalian enzyme when compared to r*Bm*AChE1. Eserine was found to be highly selective for r*Bm*AChE1 over bovine AChE (123-fold), and moderately selective over *h*AChE (46-fold). The SR of experimental carbamates for r*Bm*AChE1 were shown to be highly variable and ranged from 1-fold to 360-fold for *h*AChE and 4-fold to 338-fold for bovine AChE (Table 2). The most potent experimental inhibitor, **6**, presented the largest SR (338-fold) for bovine AChE and was also found to be very selective against *h*AChE with an SR of 342. The lowest SR observed for r*Bm*AChE1 and bovine and *h*AChE was **3**, with SR values of 4-fold and 1-fold, respectively. Coumaphos oxon was found to have SR of 104-fold and 11-fold for bovine and *h*AChE, respectively. The SR values for **6** are 3.3-fold (bovine AChE) and 31-fold (*h*AChE) better than the currently used acaricide, coumaphos oxon. PS and bivalent inhibitors were both found to be negatively selective, as they inhibited the mammalian enzyme with greater efficacy compared to r*Bm*AChE1.

The selectivity (Table 2) of the experimental carbamates comparing *h*AChE to *Pp*AChE was found to range from 23-fold (**1**) to 611-fold (**7**). Propoxur was found to be most selective standard carbamate with an SR of 21-fold, whereas **6** was found to have an SR of 366-fold, a 17-fold increase over propoxur. Edrophonium was found to be negatively selective for *Pp*AChE, whereas eserine was 7.6-fold selective, 3-fold less than the least selective experimental carbamate. PS inhibitors were found to be poorly selective, with SR values near unity (Table 2). A ten-fold difference in SR was observed between the bivalent inhibitors, with donepezil being negatively selective for *Pp*AChE and BW284c51 being non-selective (SR = 1.1).

3.4. Homology modeling and site directed mutagenesis (W384F) of rBmAChE1

Homology model of the *Bm*AChE1 was constructed, and the percentage identity of the template and target sequence was 42%. The alignment contained 8 insertions/deletions. All but one of the indels were remote from the CS/PS, with a loop three residues shorter being on the outer rim of the PS (N336-V340). Overall backbone RMSD to the template was 1.35 A. The catalytic and peripheral sites, as well as the gorge, were inspected and compared to X-ray structures of the complexes of tacrine and donepezil, using Protein Data Bank accession files PDB ID 1ACJ and PDB ID 1EVE, respectively. The model revealed that the organization of the CS, gorge, and PS was overall similar to other species, but several distinctive features were observed. Firstly, AChE from other species typically has a phenylalanine or tyrosine residue in the position corresponding to W384. Inspection of the inhibitor complex structures revealed that the phenylalanine side chain is able to adopt alternative orientations, either enlarging the catalytic site so that tricyclic ligands such as tacrine can be accommodated, or expanding the gorge when bulkier moieties are present there, as is the case with donepezil. On the other hand, larger W384 side-chain in *Bm*AChE1 fills most of the space occupied by either of the phenylalanine conformers. Another significant difference observed is that generally highly conserved tryptophan residue in the PS (W286 in human enzyme) is substituted by T335.

Inhibition potencies of AChE inhibitors to the r*Bm*AChE1 (W384F) mutant enzyme and comparison to r*Bm*AChE1 are shown in Table 4. When compared to r*Bm*AChE1 wildtype, the mutated r*Bm*AChE1 (W384F) enzyme displayed a statistically significant increase in sensitivity to tacrine, BW284c51, and donepezil. Tacrine and BW284c51 were found to be 6.4-fold and 8-fold more potent to the mutated enzyme (W384F) when compared to r*Bm*AChE1 wildtype (Table 4). Donepezil had a >40-fold increase in potency to the mutated enzyme, but an exact value could not be determined, since only 3% of the r*Bm*AChE1 wildtype enzyme was inhibited at 100 μM. Propoxur was the only carbamate AChE inhibitor to show a statistically significant increase (1.4-fold) in IC_{50} value between the wildtype and mutant enzymes. The other carbamates had activity ratios near unity (Table 4).

3.5. AChE from resistant tick strains

A number of resistant strains were collected and their AChEs cloned into cell lines and sequenced (Table 1). The strains were tested in preliminary screens against a variety of CS- and PS-directed compounds listed in Table 2, and little resistance was noted. More complete experiments were performed with compounds **1** and **6**. Compound **1** was tested because we have studied it extensively over the last few years [28], and compound **6** because it was a potent *in vitro* inhibitor of r*Bm*AChE. IC_{50} values for these strains were all in the low nanomolar range, and they generally showed little cross resistance to coumaphos oxon and experimental compounds **1** and **6**, as shown in Table 5. Exceptions were compounds **1** and **6** in the Tuxpan #11 strain, where the resistance ratios were 2.3 and 5.2, respectively, likely due to influence of the D188E and/or E196G substitutions in the Tuxpan #11 construct (Table 1).

3.6. Mammalian toxicity studies

Estimates of LD_{50} values were collected for experimental carbamates **1**, **6**, and **7**. LD_{50} estimates for compounds **1** and **6** were 154 (n = 8) and 1732 (n = 7) mg/kg, respectively. Due to low numbers of animals used, no confidence limits for these values could be accurately calculated. For compound **7**, no lethality was observed up to 2000 mg/kg (n = 2).

4. Discussion

CS-directed compounds were potent inhibitors of both enzymes, but structure–activity relationships of carbamates differ

Table 4
IC_{50} values of AChE inhibitors with the mutated r*Bm*AChE1 (W384F) enzyme compared to r*Bm*AChE1 wildtype. IC_{50} values are shown as means ($n = 3$). Letters after 95% CI values represent statistical significance for IC_{50} values between the two enzymes. Asterisks represent statistical significance at $P < 0.05$ when compared to the wild type enzyme values (Table 2).

Inhibitor	r*Bm* W384F AChE1 – IC_{50} (nM; 95% CI)	r*Bm*AChE1 IC_{50}/W384F IC_{50} ratio
Coumaphos oxon	9 (3–15)	1.1
Propoxur	47 (36–57)*	0.7
Carbofuran	6 (3–10)	0.8
Bendiocarb	18 (10–25)	0.9
BW284C51	1,570 (1481–1658)*	8.1
Tacrine	34,400 (28,200–40,800)*	6.4
Donepezil	2,298 (1385–3211)*	43.5
1	53 (36–69)	0.7
6	23 (15–31)	0.7
7	256 (244–266)	1.2

Table 5
IC_{50} values and resistance ratios in parentheses (RR = IC50 field strain/IC50 WT) for field strains of *Bm*AChE (Mean nM ± SEM, $n = 3$). Statistical significance was determined by unpaired *t*-test.

Compound	WT	San Roman #4	San Roman #11	Munoz #4	Tuxpan #11	Tuxpan #17
Coumaphos oxon	14 ± 0.6	13 ± 2 (0.93)	12 ± 0.7 (0.86)	26 ± 0.6** (1.9)	19 ± 0. 3** (1.4)	28 ± 0.6** (2)
1	45 ± 1	48 ± 2 (1.1)	70 ± 6* (1.6)	34 ± 2 (0.76)	103 ± 5** (2.3)	34 ± 2 (0.76)
6	13 ± 0.3	12 ± 0.3 (0.92)	15 ± 0.3** (1.2)	13 ± 0.3 (1)	67 ± 1.5** (5.2)	19 ± 0.3** (1.4)

* $P < 0.05$.
** $P < 0.01$.

for tick and sandfly AchE. For r*Bm*AChE1, the loss of activity observed for carbamates **2** and **3** when compared to **1** suggest the enzyme has difficulty accommodating the larger trialkylsilyl groups of **2** and **3**, and that *meta* side chains must be smaller in size to effectively inhibit the enzyme. In contrast, *Pp*AChE apparently can accommodate these groups with little loss of activity (Table 2). Potency against r*Bm*AChE1 for *ortho*- substituted phenyl methylcarbamates (**4**–**6**) was high, but they were less active than *meta*-substituted compounds when tested on *Pp*AChE. The high potency of **6** to both r*Bm*AChE1 and r*Pp*AChE is exceptional, as it is 7-fold more potent when compared to *Ag*AChE (IC_{50}: 104 nM [37]), the enzyme species it was designed to target. Compound **6** was shown to be equipotent to coumaphos oxon and possess about 3-fold and 30-fold greater selectivity than this compound over bovine AChE and *h*AChE, respectively (Table 2). Selectivity was reduced to <10-fold with *meta*-substituted side chains, suggesting the design of future *N*-methylcarbamates for *Bm* control should focus on *ortho*-substitutions. The excellent potency and selectivity of compound **6** for *Pp*AChE suggests it might be a viable control method for *Pp* populations in locations of close proximity to humans, such as insecticide-treated nets or indoor residual spraying.

r*Bm*AChE1 was found to be over 1000-fold less sensitive to tacrine when compared to all other species studied, indicating a unique catalytic site in *Bm*AChE. Molecular homology models (Fig. 2) indicate that there are two significant orthologous substitutions that inhibit ligand binding in *Bm*AChE1, W384/Y337 and T335/W286 (*Bm*/human numbering). Typically, phenylalanine or tyrosine is analogous to the W384 residue in *Bm*AChE1. In *Tc*, F330 is analogous to W384 in the tick and is thought to possess two orientations to accommodate various ligands. These two orientations are shown in Fig. 2. However, the W384 residue in *Bm*AChE1 possesses a larger side chain than Y337 in *h*AChE (F330 in *Tc*AChE). The model suggests that steric clashes of the tryptophan side chain with bulky ligands in the CS (tacrine) or gorge (donepezil) would be resolved by the re-orientation of the tyrosine side chain in AChE of other species, but cannot be completely avoided with the W384 of *Bm*AChE1. This structural clash contributes to the significantly reduced affinity of these inhibitors, although the difference in potency for tacrine can be only partially accounted for by mutation W384F (Table 4).

Presumably, the T335/W286 substitution also contributed to the reduced potency of the tacrine dimer series. Monomeric tacrine was among the least active inhibitor in the series, with *bis*(8)-tacrine being the most potent at an IC_{50} value of about 1 μM. The pattern of inhibition for r*Bm*AChE was similar to *h*AChE [38], as the IC_{50} decreased with increasing tether length to *bis*(8)-tacrine and then increased again as tether length neared 12 methylenes. The chicken enzyme is known to be missing Y70, Y121, and W270, three principal PS residues, and is therefore considered to be devoid of a PS [27]. Interestingly, r*Bm*AChE1 sensitivity was reduced compared to chicken AChE [38] and ranged from 16-fold less for *bis*(9)-tacrine to 341-fold less for *bis*(4)-tacrine, suggesting the T335/W286 substitution (*Bm*/human numbering) potentially provides a blockade effect or steric hindrance that serves to prevent adequate binding of bivalent ligands to the CS and PS sites. However, it is unlikely that the peripheral site is absent in r*Bm*AChE1, as ethidium bromide inhibited the enzyme with nearly the same potency values seen in numerous other species. Additionally, the pattern of inhibition (increased potency with increasing tether length to *bis*(8)-tacrine, then decreasing potency) likely indicates the presence of dual site binding.

The r*Pp*AChE enzyme yielded different responses to the tacrine series of compounds when compared to r*Bm*AChE1, *Ag*AChE, and *h*AChE. The monomeric tacrine was found to be among the least potent of the tacrine dimer series, but was similar in potency to every species studied (ca. 200 nM), excluding *Bm*AChE. However, the pattern of inhibition was different from r*Bm*AChE1, as the IC_{50} decreased with increasing tether length, but did not increase again as the tether linkage increased to 12 methylenes. *Drosophila melanogaster* AChE, an *ace-2* encoded enzyme, has also been shown to have this pattern of inhibition to the tacrine dimer series [38]. Insects utilizing the *ace-2* gene to encode functional AChE may likely possess a different protein structure than *ace-1* insects that is capable of accommodating larger tether lengths over shorter tethers.

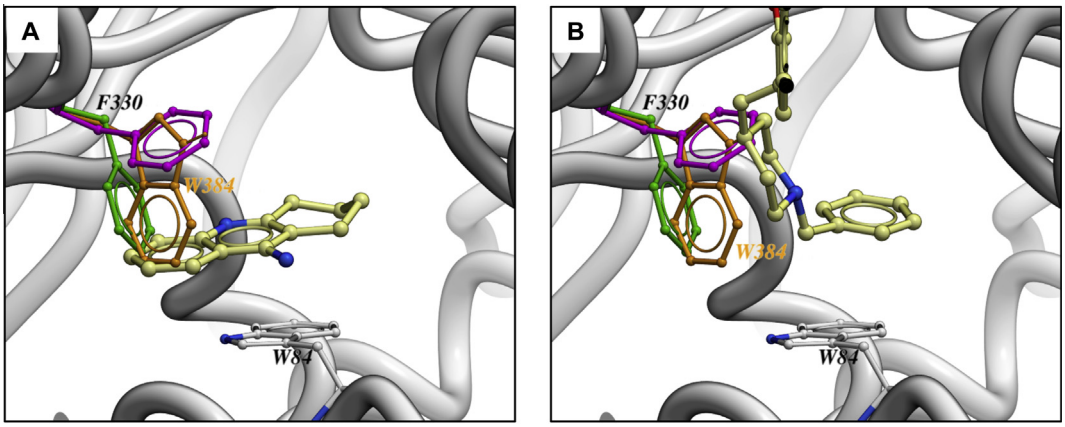

Fig. 2. Superposition views of tacrine (A) and donepezil (B) complexes onto the model of *Bm*AChE1. F330 is shown to exist in two orientations: (A) conformation adopted in complex with tacrine is shown in magenta, and (B) the conformation adopted in complex with donepezil is shown in green. Structural clash of both ligands with W384 (orange) is shown, along with conserved W84 at the bottom of the active site for orientation. (For interpretation of the references to colour in this figure legend, the reader is referred to the web version of this article.)

In an effort to validate the homology models, site directed mutagenesis was performed to study the effect the W384/Y337 substitution has on the inhibitor potency to the r*Bm*AChE1 enzyme. The mutation performed was W384F, since phenylalanine possesses a smaller structural size when compared to tryptophan and a closer resemblance to tyrosine, which is found in the majority of other enzymes, including *h*AChE. Statistically significant increases in potency were observed with tacrine and the two bivalent inhibitors, BW284c51 and donepezil. Although the increase in potency to the mutated enzyme with tacrine and bivalent inhibitors validates the model of W384 preventing access of larger ligands to the acyl site, it does not fully account for the decreased r*Bm*AChE1 sensitivity, as the W384F mutation did not decrease the IC_{50} values to those observed in other species. One would expect an additional 172-fold increase in potency for tacrine if the mutation accounted for all of the decreased inhibitor potency. Therefore, it is plausible to suggest other orthologous substitutions are present in conjunction with W384/Y337 (*Bm*/human numbering), allowing for a unique *Bm*AChE1 gorge geometry and therefore, a constricted entry to the acyl site. For instance, molecular homology models suggest the T335/W286 (*Bm*/human numbering) substitution in the *Bm* peripheral site could account for a reduced sensitivity to peripheral site and bivalent inhibitors. The T335/W286 substitution in r*Bm*AChE1 could potentially disrupt the transient binding mechanism of the PS [25] and effectively reduce the potency of acyl site inhibitors through allosteric effects at the CS.

Resistant strain enzymes utilizing a number of additional mutations (Table 1) were analyzed for sensitivity to experimental carbamates. In general, these studies observed little cross resistance to either coumaphos or carbamates (Table 5), and would not be expected to cause field use failures. An exception was Tuxpan #11, which showed about 5-fold resistance to **6** at the enzyme level, and might indicate incipient resistance to this molecule. This strain carries four mutations, two of which (D188G and E196G) are unique to Tuxpan #11. It would be appropriate in future studies to analyze further the distribution and impact of these mutations on resistance.

Mouse toxicity data for propoxur, a WHO-approved carbamate for mosquito control, has a mammalian LD_{50} of 24 mg/kg using methods essentially identical to those employed here [39]. Thus, it was sixfold more toxic than compound **1** (154 mg/kg) to mice. The presence of longer side chains containing a sulfur or oxygen atom in the *ortho* position, as seen in **6** and **7**, decreased the mammalian toxicity by at least 70-fold when compared to propoxur, consistent with their reduced activity against mammalian enzymes (Table 2). These data suggest the novel carbamates would be substantially safer than the currently utilized methylcarbamates in pest control applications, if they provide equal or better *in vivo* toxicity to pest species at similar application rates.

Acknowledgments

We thank the National Institutes of Health (AI082581), the Foundation for the National Institutes of Health (GCGH-1497) through the Grand Challenges in Global Health Initiative, the United States Department of Agriculture (Specific Cooperative Agreement 108-0128-098) and Deployed War-fighter Protection Research Program, as well as Virginia Tech (the College of Science, the Department of Chemistry, and Fralin Life Science Institute) for financial support of this work. We would also like to thank Kristie Schlechte for excellent technical assistance with the tick recombinant enzymes, and Dr. James Mutunga for his part of the mouse oral toxicity studies. The USDA is an equal opportunity provider and employer.

References

[1] J. Hemingway, H. Ranson, Insecticide resistance in insect vectors of human disease, Ann. Rev. Entomol. 45 (2000) 369–389.
[2] O. Graham, J. Hourrigan, Eradication programs for the arthropod parasites of livestock, J. Med. Entomol. 6 (1977) 629–658.
[3] N. Jonsson, D. Mayer, A. Matschoss, P. Green, J. Ansell, Production effects of cattle tick (*Boophilus microplus*) infestation of high yielding dairy cows, Vet. Parisitol. 78 (1998) 65–77.
[4] P. Desjeux, The increase in risk factors of leishmaniasis worldwide, T. Roy. Soc. Trop. Med. Hyg. 95 (2001) 239–245.
[5] R. Miller, R. Davey, J. George, First report of organophosphate-resistant *Boophilus microplus* (Acari: Ixodidae) within the United States, J. Med. Entomol. 42 (2005) 912–917.
[6] J. George, J. Pound, R. Davey, Chemical control of ticks on cattle and the resistance of these parasites to acaricides, Parasitol 129 (2004) S353–S366.
[7] M. Maroli, R. Lane, The effect of permethrin-impregnated curtains against phlebotomine sandflies: laboratory and field studies, Parasitol 33 (1991) 399–404.
[8] M. Mutinga, M. Basimike, C. Mutero, A. Ngindu, The use of permethrin impregnated wall cloth for control of vectors of malaria and leishmaniasis in Kenya – II. Effect of phlebotomine sandfly populations, Insect Sci. Appl. 13 (1992) 163–172.
[9] B. Alexander, M. Usma, H. Cadena, B. Quesada, Y. Solarte, W. Roa, B. Travi, Evaluation of deltamethrin impregnated bednets and curtains against phlebotomine sandflies in Valle del Cauca, Columbia, Med. Vet. Entomol. 9 (1995) 279–283.
[10] T. Morsy, R. Aboul Ela, B. El Gozamy, M. Salama, D. Ragheb, Residual effect of four insecticides applied for indoor control of *Phlebotomus papatasi* (Scopoli), J. Egyp. Soc. Parisitol 23 (1993) 485–492.

[11] A. Falcao, A. Falcao, C. Pinto, C. Gontijo, A. Flaqueto, Effect of deltametrin spraying on the sandfly populations in a focus of American cutaneous leismaniasis, Mem. Inst. Oswaldo Cruz 4 (1991) 399–404.
[12] S. Surendran, S. Karunaratne, Z. Adams, J. Hemingway, N. Hawkes, Molecular and biochemical characterization of a sand fly population from Sri Lanka, Evidence for insecticide resistance due to altered esterases and insensitive acetylcholinesterase, Bull. Entomol. Res. 95 (2005) 371–380.
[13] R. Jamroz, F. Guerrero, J. Pruett, D. Oehler, R. Miller, Molecular and biochemical survey of acaricide resistance mechanisms in larvae from Mexican strains of the southern cattle tick, *Boophilus microplus*, J. Insect Physiol. 46 (2000) 685–695.
[14] W. Roulston, H. Schnitzerling, C. Schuntner, Acetylcholinesterase insensitivity in the Biarra strain of the cattle tick *Boophilus microplus*, as a cause of resistance to organophosphorous and carbamate acaricides, Aust. J. Biol. Sci. 21 (1968) 759–767.
[15] R. O'Brien, Insecticides action and metabolism, Academic Press, New York, 1967.
[16] A. Li, R. Davey, R. Miller, J. George, Resistance to Coumaphos and Diazinon in *Boophilus microplus* (Acari: Ixodidae) and evidence for the involvement of an oxidative detoxification mechanism, J. Med. Entomol. 40 (2003) 482–490.
[17] C. Schuntner, W. Roulston, H. Schnitzerling, A mechanism of resistance to organophosphorous acaricides in a strain of the cattle tick, *Boophilus microplus*, Aust. J. Biol. Sci. 21 (1968) 97–109.
[18] R. Rosario-Cruz, F. Guerroro, R. Miller, R. Rodriguez-Vivas, D. Dominguez-Garcia, A. Cornel, Roles played by esterase activity and by a sodium channel mutation involved in pyrethroid resistance in populations of *Boophilus microplus* (Acari: Ixodidae) collected from Yucatan, Mexico, J. Med. Entomol. 42 (2005) 1020–1025.
[19] J. Morgan, S. Corley, L. Jackson, A. Lew-Tabor, P. Moolhuijzen, N. Jonsson, Identification of a mutation in the *para*-sodium channel gene of the cattle tick *Rhicephalus (Boophilus) microplus* associated with resistance to synthetic pyrethroid acaricides, Int. J. Parisotol 39 (2009) 775–779.
[20] J. Sussman, M. Harel, F. Frolow, C. Oefner, A. Goldman, L. Toker, I. Silman, Atomic Structure of acetylcholinesterase from *Torpedo californica:* a prototypical acetylcholine-binding protein, Science 253 (1991) 872–879.
[21] M. Harel, G. Kryger, T. Rosenberry, W. Mallender, T. Lewis, R. Fletcher, J. Cuss, I. Silman, J. Sussman, Three-dimensional structures of *Drosophila melanogaster* acetylcholinesterase and of its complexes with two potent inhibitors, Prot. Sci. 9 (2000) 1063–1072.
[22] Y. Bourne, P. Taylor, P. Bougis, P. Marchot, Crystal structure of mouse acetylcholinesterase: A peripheral site-occluding loop in tetrameric assembly, J. Biol. Chem. 5 (1999) 2963–2970.
[23] M. Harel, I. Schalk, L. Ehret-sabatier, F. Bouet, M. Geldner, C. Hirth, P. Axelsen, I. Silman, J. Sussman, Quaternary ligand binding to aromatic residues in the active-site of acetylcholinesterase, Proc. Nat. Acad. Sci. USA 90 (1993) 9031–9035.
[24] T. Szegletes, W. Mallender, P. Thomas, T. Rosenberry, Substrate binding to the peripheral site of acetylcholinesterase initiates enzymatic catalysis: Substrate inhibition arises as a secondary effect, Biochemistry 38 (1999) 122–133.
[25] W. Mallender, T. Szegletes, T. Rosenberry, Acetylthiocholine binds to Asp74 at the peripheral site of human acetylcholinesterase as the first step in the catalytic pathway, Biochemistry 39 (2000) 7753–7763.
[26] Z. Radic, P. Taylor, Structure and function of cholinesterases, in: Toxicology of Organophosphate and Carbamate Compounds, Elsevier Inc., Academic Press, 2006.
[27] J. Eichler, A. Anselmet, J. Sussman, J. Massoulie, I. Silman, Differential effects of "peripheral" site ligands on *Torpedo* and chicken acetylcholinesterase, Mol. Pharmacol. 45 (1993) 335–340.
[28] J.A. Hartsel, D.M. Wong, J.M. Mutunga, M. Ma, T.D. Anderson, A. Wysinski, R. Islam, E.A. Wong, S.L. Paulson, J. Li, P.C.-H. Lam, M. Totrov, J.R. Bloomquist, P.R. Carlier, Re-engineering aryl methylcarbamates to confer high selectivity for inhibition of *Anopheles gambiae* vs human acetylcholinesterase, Bioorg. Med. Chem. Lett. 22 (2012) 4593–4598.
[29] P. Carlier, Y. Han, E. Chow, C. Li, H. Wang, T. Lieu, H. Wong, Y. Pang, Evaluation of short-tether Bis-THA AChE inhibitors: A further test of the dual binding site hypothesis, Bioorg. Med. Chem. 7 (1999) 351–357.
[30] G. Ellman, K. Courtney, V. Andres, R. Featherstone, A new rapid colorimetric determination of acetylcholinesterase activity, Biochem. Pharmacol. 7 (1961) 88–95.
[31] R. Abagyan, E. Rausch, M. Totrov, ICM Manual, Molsoft 2011, http://www.molsoft.com/man/.
[32] R. Abagyan, M. Totrov, Biased probability Monte Carlo conformational searches and electrostatic calculations for peptides and proteins, J. Mol. Biol. 235 (1994) 983–1002.
[33] K. Temeyer, J. Pruett, P. Olafson, Baculovirus expression, biochemical characterization and organophosphate sensitivity of rBmAChE1, rBmAChE2, and rBmAChE3 of *Rhipicephalus (Boophilus) microplus*, Vet. Parasitol. 172 (2010) 114–121.
[34] K. Temeyer, P. Olafson, D. Brake, A. Tuckow, A. Li, A. Pérez de León, Acetylcholinesterase of *Rhipicephalus (Boophilus) microplus* and *Phlebotomus papatasi*: Gene identification, expression, and biochemical properties of recombinant proteins, *Pestic. Biochem. Physiol.*, this issue.
[35] K. Temeyer, D. Brake, A. Tuckow, A. Li, A. Perez de Leon, Acetylcholinesterase of the sand fly, *Phlebotomus papatasi* (Scopoli): cDNA sequence, baculovirus expression, and biochemical properties, *Parasit. Vectors* **6**, 2013, 31.
[36] R. Bruce, An up-and-down procedure for acute toxicity testing, Fundam. Appl. Toxicol. 5 (1985) 151–157.
[37] Y. Jiang, D. Swale, P. Carlier, J. Hartsel, M. Ma, F. Ekström, and J. Bloomquist, Evaluation of novel carbamate insecticides for neurotoxicity to non-target species, *Pestic. Biochem. Physiol*., this issue.
[38] T. Anderson, S. Paulson, D. Wong, P. Carlier, J. Bloomquist, Pharmacological mapping of the acetylcholinesterase catalytic gorge in mosquitoes with Bis(*n*)-tacrines, in: J. Clark (Ed.), Advances in Human Vector Control, ACS Symposium Series, American Chemical Society, Washington, DC, 2009.
[39] A. Black, Y. Chiu, M. Fahmy, T. Fukuto, Selective toxicity of N-sulfenylated derivatives of insecticidal methylcarbamate esters, J. Agri. Food Chem. 21 (1973) 747–751.